Determining Geometrical Spreading from Traveltimes in Anisotropic Media

Claudia Vanelle and Dirk Gajewski

email: *vanelle@dkrz.de*

keywords: *Geometrical Spreading, Anisotropy, Traveltimes, Interpolation, Migration, Amplitudes*

ABSTRACT

Geometrical spreading plays an important role for amplitude preserving migration, which is a very time-consuming process. In order to achieve efficiency in terms of computational time and, particularly, storage space, we propose a method to determine geometrical spreading for any wave type in anisotropic media from coarsely-gridded traveltime tables. The method is based on a hyperbolic traveltime expansion and provides also a fast and accurate algorithm for the interpolation of traveltimes, including the interpolation of complete shots. Examples demonstrate the applicability of the method to arbitrary 3D anisotropic media.

INTRODUCTION

Geometrical spreading, together with traveltimes, plays an important role in many applications of reflection seismology, such as migration, inversion, and modelling. The traditional method of computing geometrical spreading in anisotropic media is to perform dynamic ray tracing (Gajewski and Pšenčík, 1990). Other fast methods based on finite-difference eikonal solvers (e.g. Pusey and Vidale, 1991) or a direct solution of the transport equation with finite differences (Buske, 2000) were proposed for isotropic media only. Methods to determine the spreading directly from traveltimes were presented by Vidale and Houston (1990) and Vanelle and Gajewski (1999), but again, only for isotropic media.

In this paper we introduce a technique for the determination of geometrical spreading from traveltimes in media with arbitrary anisotropy. Like the method presented in Vanelle and Gajewski (1999) it is based on the coefficients of a hyperbolic traveltime expansion. Regarding application to amplitude preserving migration the new technique has a strong advantage compared to dynamic ray tracing: whereas with dynamic ray tracing the spreading has to be stored for the computation of the weight functions (in addition to the traveltimes required for the diffraction time surfaces and several other quantities like, e.g, the ray angles), this is not necessary if the spreading, angles, etc. can be determined directly from traveltimes. At the same time, our method allows the reduction of storage space because the hyperbolic traveltime equation also provides a technique for the fast and accurate traveltime interpolation from coarse grids onto the required fine migration grids, including the possibility to interpolate between sources.

The method is particularly useful in combination with a procedure for the computation of coarsely-gridded traveltimes (Gajewski et al., 2002), as, e.g., the wave front construction techniques introduced by Vinje et al. (1993). In contrast to methods based on finite-difference eikonal solvers these techniques also yield later arrival traveltimes, that are required for imaging of complex structures (Geoltrain and Brac, 1993).

After a brief introduction to the hyperbolic traveltime formula, we establish the relationship between the coefficients of the hyperbolic formula and the geometrical spreading in arbitrary anisotropic media,

including a description of our implementation. This is followed by several examples, first on the interpolation of anisotropic traveltimes, and then for the determination of spreading from traveltimes in anisotropic media. To estimate the accuracy of the method, it is also applied to a model where an analytic solution exists. Finally, we will conclude our results.

METHOD

The General Move-out Relation

The method is based on the hyperbolic traveltime equation introduced in Vanelle and Gajewski (2002a). It follows from a Taylor expansion of the squared traveltime T^2. The expansion is carried out in the three components of the source position vector, $\hat{\mathbf{s}} = (s_1, s_2, s_3)$ and those of the receiver position, $\hat{\mathbf{g}} = (g_1, g_2, g_3)$. The expansion point is denoted by $(\hat{\mathbf{s}}_0, \hat{\mathbf{g}}_0)$. The hyperbolic equation reads

$$T^2(\hat{\mathbf{s}}, \hat{\mathbf{g}}) = (T_0 - \hat{\mathbf{p}}_0 \triangle\hat{\mathbf{s}} + \hat{\mathbf{q}}_0 \triangle\hat{\mathbf{g}})^2 + T_0 \left(-\triangle\hat{\mathbf{s}}^\top \underline{\hat{\mathbf{S}}} \triangle\hat{\mathbf{s}} + \triangle\hat{\mathbf{g}}^\top \underline{\hat{\mathbf{G}}} \triangle\hat{\mathbf{g}} - 2\triangle\hat{\mathbf{s}}^\top \underline{\hat{\mathbf{N}}} \triangle\hat{\mathbf{g}} \right) \quad , \qquad (1)$$

where T_0 is the traveltime in the expansion point. The vectors $\triangle\hat{\mathbf{s}} = \hat{\mathbf{s}} - \hat{\mathbf{s}}_0$ and $\triangle\hat{\mathbf{g}} = \hat{\mathbf{g}} - \hat{\mathbf{g}}_0$ are the deviations of the source and receiver positions ($\hat{\mathbf{s}}$ and $\hat{\mathbf{g}}$) from the location of the expansion point ($\hat{\mathbf{s}}_0$ and $\hat{\mathbf{g}}_0$). The first-order derivatives

$$p_{0_i} = -\frac{\partial T}{\partial s_i} \quad \text{and} \quad q_{0_i} = \frac{\partial T}{\partial g_i} \qquad (2)$$

are the slowness vectors at the source and the receiver, and the matrices

$$S_{ij} = -\frac{\partial^2 T}{\partial s_i \partial s_j} \quad , \quad G_{ij} = \frac{\partial^2 T}{\partial g_i \partial g_j} \quad , \quad \text{and} \quad N_{ij} = -\frac{\partial^2 T}{\partial s_i \partial g_j} \quad , \qquad (3)$$

$(i, j = 1, 2, 3)$ are the second-order derivatives of the traveltimes, which are closely related to the curvature of the wavefront.

The hyperbolic traveltime approximation given by Equation (1) is a universal expression. During the last years the authors have shown its usefulness for a variety of applications: In Vanelle and Gajewski (2002a) it is applied to the interpolation of traveltimes in arbitrary 3-D isotropic media including the interpolation of the source position. The coefficients from Equation (1) were further used for the computation of geometrical spreading from traveltimes in isotropic media (Vanelle and Gajewski, 1999). In Vanelle and Gajewski (2002b), the hyperbolic formula is applied to determine weight functions for amplitude preserving Kirchhoff migration in isotropic media, and for the optimisation of the migration aperture (Vanelle and Gajewski, 2001). Equation (1) is also valid for reflected events and poses an extension of the well-known $T^2 - X^2$ method to arbitrary 3-D media (Gajewski and Vanelle, 2001). Therefore it can be considered to be a move-out relation of second order in the most general form (Gajewski and Vanelle, 2002).

Since no assumptions on the model were made for the derivation of Equation (1) it is equally valid in isotropic as in anisotropic media for any wave type (i.e. quasi shear and quasi compressional waves). If suitable traveltime tables (i.e. for different source and receiver combinations) are available, the coefficients of Equation (1) can be directly determined from these traveltimes, which need only be given on coarse grids. In this case of coarsely-sampled input traveltimes, the locations of the coarse grid-points correspond to the expansion points. Although the method is equally valid for reflection traveltimes, we suggest here to apply it to migration. In that case, diffraction traveltime tables must exist in any event for the determination of the Huygens surface, along which the traces are stacked. Therefore, we will from now on focus on diffraction traveltimes. We give an example for the determination of the coefficients: the coefficients q_{0_1} and G_{11} can be computed from the three traveltime values $T_0 = T(\hat{\mathbf{s}}_0, \hat{\mathbf{g}}_0)$, $T_1 = T(\hat{\mathbf{s}}_0, \hat{\mathbf{g}}_0 - \triangle g_1)$, and $T_2 = T(\hat{\mathbf{s}}_0, \hat{\mathbf{g}}_0 + \triangle g_1)$, where $\triangle g_1$ is the coarse grid-spacing in the direction of the g_1 component. The traveltimes T_1 and T_2 are inserted into the hyperbolic equation (1), leading to two equations for two unknowns, which can be solved for q_{0_1} and G_{11}. The result is

$$q_{0_1} = \frac{T_2^2 - T_1^2}{4T_0 \triangle g_1} \quad \text{and} \quad G_{11} = \frac{T_2^2 + T_1^2 - 2T_0^2}{2T_0 \triangle g_1^2} - \frac{q_{0_1}^2}{T_0} \quad . \qquad (4)$$

The remaining coefficients can be determined in the same way by using the appropriate traveltime combinations. This is explained in more detail in Vanelle and Gajewski (2002a).

For the determination of derivatives with respect to the third (z) component of the source coordinates from traveltimes, however, additional traveltime tables are required for source positions buried in the subsurface, below the registration surface. If such tables are available, these coefficients can be determined in the same fashion as by Equation (4). An alternative to the generation of these traveltime tables is to assume that the source is located in an isotropic layer. In that case, the isotropic eikonal equation can be used to express the z derivatives of the traveltimes without further need for additional traveltime tables. Please refer to Vanelle and Gajewski (2002a) for the resulting equations for these coefficients.

If all coefficients are determined, Equation (1) can be directly applied for the traveltime interpolation onto fine grids. It is even possible to interpolate finely-gridded traveltime tables between sources, i.e. $\Delta \hat{s} \neq 0$, because the derivatives with respect to the source position are also known. Since the curvature of the wavefront is accounted for by the second-order traveltime derivatives, the hyperbolic interpolation is superior to the commonly-used trilinear interpolation (Vanelle and Gajewski, 2002a). An example on the hyperbolic traveltime interpolation in an anisotropic medium will be given below.

Geometrical Spreading

A wavefront is described by a surface with $T = const$. This means that the traveltime equation (1) translates into an expression for the local wavefront in the vicinity of the expansion point, where the wavefront is approximated with a surface of second order. The curvature of the wavefront determines the relative geometrical spreading L. Since the curvature of a surface can be described by its second-order derivatives it is possible to establish a relationship between the geometrical spreading and the mixed second-order derivative matrix $\underline{\hat{N}}$ (cf. Equation (3)). Following standard ray theory (e.g. Červený, 2001), the geometrical spreading for a point source is evaluated in terms of the 2×2 matrix $\underline{\mathbf{Q}}_2$ which describes the divergence of the ray tube for point source initial conditions. For details, please refer to Červený (2001). The modulus of the relative geometrical spreading is given by (Červený, 2001)

$$L = \sqrt{|\det \underline{\mathbf{Q}}_2|} \tag{5}$$

The matrix $\underline{\mathbf{Q}}_2$, and hence the geometrical spreading L, are usually computed by dynamic ray tracing. In this paper, however, we do not apply dynamic ray tracing, but use the relationship between the matrix $\underline{\mathbf{Q}}_2$ and the matrix $\underline{\mathbf{N}}$, which is the upper left 2×2 sub-matrix of $\underline{\hat{N}}$, (to distinguish between 2×2 and 3×3 matrices, the latter carry a hat symbol). This relationship was derived by Schleicher et al. (2001) and leads to

$$|\det \underline{\mathbf{Q}}_2| = \frac{\cos \alpha_s \cos \alpha_g}{\cos \chi_s \cos \chi_g} \, |\det \underline{\mathbf{N}}|^{-1} \quad . \tag{6}$$

In Equation (6), α_s (α_g) is the angle between the ray or group velocity vector $\hat{\mathbf{v}}_s$ ($\hat{\mathbf{v}}_g$) and the s_3 (g_3) direction. The angle χ_s (χ_g) is made by the ray velocity vector and the slowness vector $\hat{\mathbf{p}}$ ($\hat{\mathbf{q}}$). It is given by the relationship

$$\cos \chi_s = \frac{V_s}{v_s} \quad , \tag{7}$$

and for $\cos \chi_g$ accordingly, where V_s (V_g) is the phase velocity at the source (receiver), which can be determined from the slowness components by $V_s^{-2} = \hat{\mathbf{p}} \cdot \hat{\mathbf{p}}$ ($V_g^{-2} = \hat{\mathbf{q}} \cdot \hat{\mathbf{q}}$). Thus, the relative geometrical spreading becomes

$$L = \sqrt{\frac{\cos \alpha_s \, \cos \alpha_g}{|\det \underline{\mathbf{N}}|} \frac{v_s}{V_s} \frac{v_g}{V_g}} \quad . \tag{8}$$

In isotropic media, $V = v$, and Equation (8) reduces to the result derived by Hubral et al. (1992), and applied in Vanelle and Gajewski (1999) and Vanelle (2002).

The components v_{s_i} (i=1,2,3) of the ray velocity vector for an arbitrary anisotropic medium can be computed from the slowness vector $\hat{\mathbf{p}}$ and the values of density normalised elasticity tensor a_{ijkl} at the source position (Červený, 2001):

$$v_{s_i} = a_{ijkl}\, p_l\, \frac{D_{jk}}{D} \quad . \tag{9}$$

In Equation (9) the p_l are the components of the slowness vector. The matrix elements D_{jk} are given by (Červený, 2001)

$$D_{jk} = \frac{1}{2}\, \epsilon_{jlm}\epsilon_{kno}(\Gamma_{ln} - \delta_{ln})(\Gamma_{mo} - \delta_{mo}) \quad , \tag{10}$$

where

$$\Gamma_{jk} = a_{ijkl}\, p_j\, p_l \tag{11}$$

is the Christoffel matrix. Furthermore,

$$D = D_{ii} \quad . \tag{12}$$

In Equations (9) to (12) summation convention is applied. The symbol ϵ_{jlm} denotes the Levi-Civitta tensor, and δ_{jk} is Kronecker's delta. Application of Equation (9) using the slowness vector and the elasticity tensor at the source and the receiver, respectively, leads to both ray velocities, v_s and v_g, as well as to the ray angles, α_s and α_g.

Equation (9) is following from the solution of the eigenvalue problem for the Christoffel matrix Γ_{jk}. If the Christoffel matrix is degenerate, Equation (9) cannot be applied since then D=0. This happens globally in isotropic media (where, however, the velocity is known) and can also occur locally in anisotropic media for quasi shear waves. The problems with the resulting singularities are inherent to standard anisotropic high frequency methods and not a deficiency of our method in particular.

Equation (5) gives the *modulus* of the geometrical spreading. For the computation of proper migration weights, however, the phase shift due to caustics must also be considered. This is only possible, if later arrival traveltimes are available. These are important for migration in complex media (Geoltrain and Brac, 1993). Our method can also be applied to later arrivals (for an outline, see Vanelle, 2002). It has the advantage that it does not require continuous second-order derivatives of the elastic parameters, as, e.g., dynamic ray tracing does (Červený, 2001).

Using the coefficients from Equation (1) and the elasticity tensor we can now compute geometrical spreading for any wave type from coarsely-gridded traveltimes. This is a key ingredient for the computation of true-amplitude migration weight functions. For this application the determination of the spreading from traveltimes has a large advantage in storage space compared to computing geometrical spreading via dynamic ray tracing: Additional quantities like the ray angles are also required for the weight functions. These can also be computed with ray tracing, but need additional storage space, which can, for a large survey, by far exceed the existing storage capabilities. This is not necessary with the traveltime-based approach, where the complete Greens function can be determined on the fly from the traveltime coefficients. Therefore this approach is particularly suited for the application to amplitude preserving migration. Another major improvement for any type of Kirchhoff migration is the application of the hyperbolic traveltime interpolation for computing the stacking surface. This is especially valid for anisotropic media, where the computation of the Greens functions is even more time-consuming than in isotropic media. To demonstrate the capability of the method, we will now give an example on the traveltime interpolation, followed by examples on the determination of geometrical spreading in anisotropic media.

APPLICATIONS

Traveltime Interpolation

Since the hyperbolic equation does not depend on the type of model under consideration, the traveltime interpolation using Equation (1) is expected to yield results of the same order of accuracy for anisotropic media as for isotropic media. A thorough investigation of the accuracy was already carried out for isotropic

Traveltime errors for the lens model

Δs = 0 m

Traveltime errors for the lens model

Δs = 50 m
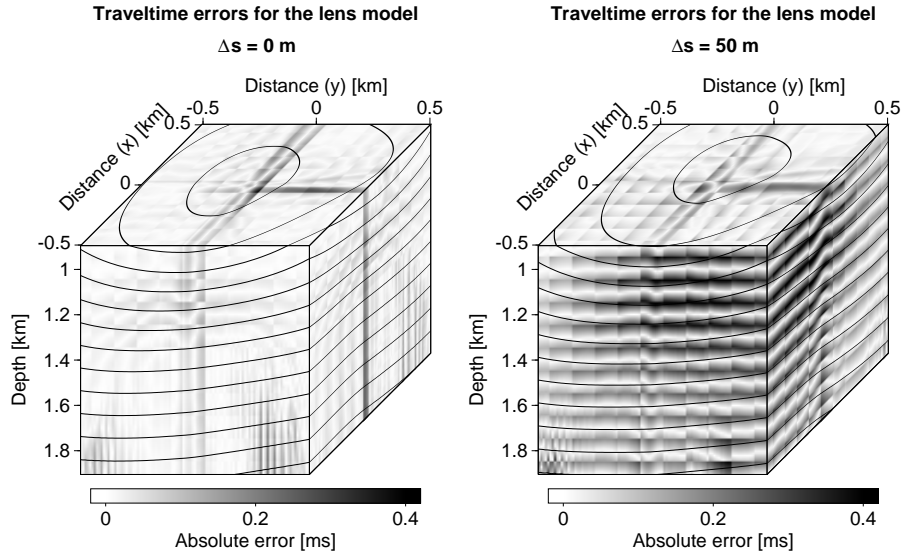
Figure 1: Traveltime errors from the hyperbolic interpolation for the velocity lens model. Values are given in milliseconds. Left: traveltime errors for the original source position at (0 m, 0 m, 0m). Right: traveltime errors for an interpolated source at (50 m, 50 m, 0m). Isochrones illustrate the un-interpolated wavefronts. The cross-shaped error distribution centred at the distances of 0 km is caused by errors in the finely-gridded reference traveltimes due to the Vidale scheme. The pattern near the edges of both cubes at higher depths are caused by ripples in the reference traveltimes.

media in Vanelle and Gajewski (2002a). Therefore we restrict ourselves to one example for the interpolation of traveltimes in anisotropic media here. Our model is a factorised medium consisting of a velocity lens. It is embedded in a medium with triclinic symmetry that corresponds to Vosges sandstone (Mensch and Rasolofosaon, 1997). The elasticity tensor of that medium is (values are given in km^2/s^2):

$$
\underline{\mathbf{A}} = \begin{pmatrix}
6.77 & 0.62 & 1.00 & -0.48 & 0.00 & -0.24 \\
 & 4.95 & 0.43 & 0.38 & 0.67 & 0.52 \\
 & & 5.09 & -0.28 & 0.09 & -0.09 \\
 & & & 2.35 & 0.09 & 0.00 \\
 & & & & 2.45 & 0.00 \\
 & & & & & 2.88
\end{pmatrix} . \tag{13}
$$

P-wave transmission traveltime tables were computed on a 10 m fine grid using a finite-difference eikonal solver in the implementation of Soukina et al. (2001). Their technique combines a Vidale scheme (Vidale, 1990) with perturbation method. Traveltimes were generated for sources in the top surface (see also Figure 1). The original traveltimes were resampled to input traveltime tables on a 100 m coarse grid. The distances between the source positions for the individual traveltime tables were also 100 m in either direction. The coefficients in Equation (1) were computed from these coarsely-gridded traveltimes and used for the interpolation onto a 10 m fine grid. The interpolated values were then compared to the original finely-gridded traveltimes and an error analysis was performed. We have considered two cases. In the first experiment, traveltimes from a source fixed at the original source position ($\hat{\mathbf{s}} = \hat{\mathbf{s}}_0$) were interpolated using the coefficients $\hat{\mathbf{q}}_0$ and $\underline{\hat{\mathbf{G}}}$. In a second experiment, we have interpolated traveltimes for a source at the position $\hat{\mathbf{s}} = \hat{\mathbf{s}}_0 + (50 \text{ m}, 50 \text{ m}, 0 \text{ m})$. This second experiment required the complete set of coefficients from Equation (1) except for the derivatives with respect to the z-component of the source position since the depth location of the source remained unchanged. The resulting traveltime errors for these two cases are displayed in Figure 1.

The median of the relative error for the interpolation to receivers only is 0.015 %, corresponding to

Traveltime errors for the lens model
$\Delta s = 0$ m

Traveltime errors for the lens model
$\Delta s = 50$ m
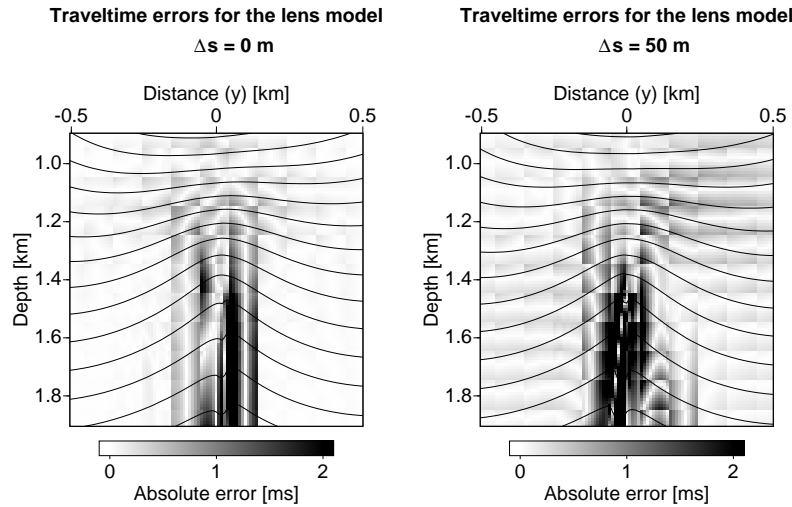
Figure 2: Traveltime errors from hyperbolic interpolation for a section through the lens model, on the left for the original source position, on the right the source position was also interpolated. The sections were extracted at the distance $x = 0$ km. The isochrones indicate the positions of triplications of the wavefront, leading to errors in the traveltime interpolation if only first-arrival traveltimes are considered. The shape of the triplicated wavefront at higher depth in the right figure is caused by artifacts in the reference traveltimes.

0.044 ms. If the position of the source is also interpolated, the median of the relative error becomes 0.041 % (0.119 ms). Owing to numerical artifacts in the reference traveltime tables (e.g. grid-points with zero traveltime), we do not give maximum errors here since these would not correctly reflect the accuracy of the method. Also, we have chosen the median instead of the average error because it is more stable concerning outliers. As we show in the next figure, Figure 2, the higher errors in some regions are not due to the method itself. Figure 2 displays the traveltime errors for both experiments in a section through the centre of the model. It illustrates that high errors occur only in the vicinity of "kinks" in the isochrones. In these regions, the assumption of continuous first- and second-order derivatives (the condition for a Taylor expansion) is not fulfilled. The "kinks" are manifestations of triplications of the wavefront. If later-arrival traveltimes are available, it is possible to interpolate the left and right branches of the traveltime curve individually (Vanelle, 2002). Then the errors in these regions reduce to the same magnitude as in the rest of the model. Since a finite-difference scheme was used for the generation of the input traveltimes, later arrivals were not available. Apart from these regions high accuracy is achieved.

If the ratio of the coarse grid spacing to fine grid spacing is 10, as in our example, the size of each traveltime table can be reduced by a factor of 10^3 (compared to no interpolation at all) if only receiver interpolation is considered. If we also take the interpolation of sources into account, the savings rise to a factor of 10^5 (assuming that the sources lie in the x-y-surface only), because less traveltime tables need to be stored. At the same time, the method has high potential savings in CPU time. In isotropic media, the interpolation of one shot in a 3D model required less than 15 % of the time needed by a fast finite-difference eikonal solver (Vanelle and Gajewski, 2002a). In anisotropic media we cannot quantify the time savings because the algorithm of Soukina et al. (2001) was used in a version which needs a large amount of time for the preparation of the model, that will be done in a separate stage in the future (Soukina, personal communication). Since traveltime generation in anisotropic media is, however, generally more time-consuming than in isotropic media, we are confident that the efficiency of our technique will be even better for anisotropic media.

**Geometrical spreading
for the elliptical model**

**Geometrical spreading errors
for the elliptical model**
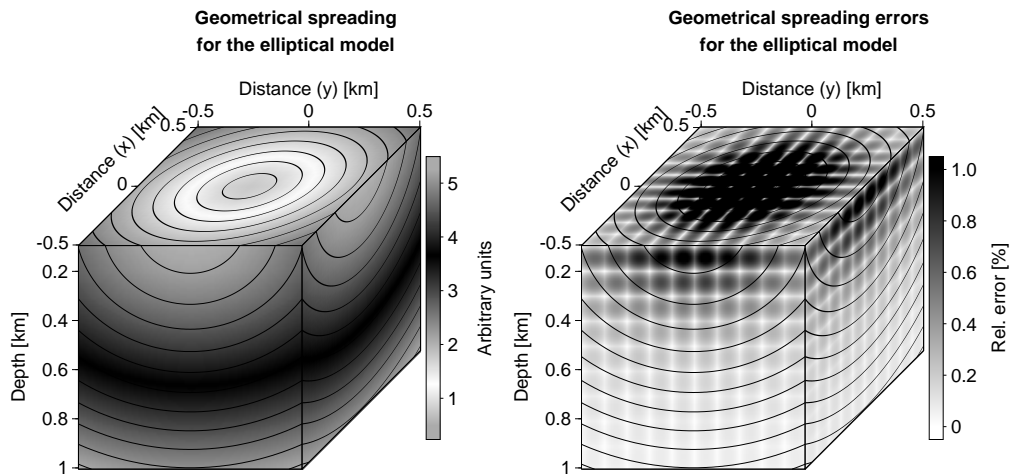
Figure 3: Geometrical spreading determined from traveltimes for a homogeneous model with elliptical symmetry (left) and errors of the geometrical spreading for this model. Relative errors are higher in the near-source vicinity because of the stronger local curvature and the trilinear interpolation onto the fine grid. Please note that the major contributions to the errors come from the trilinear interpolation, whereas at the coarse grid-points the errors are of a smaller magnitude.

Geometrical Spreading

In this section we give examples for two models, a homogeneous model with elliptical anisotropy where an analytic solution exists, and the triclinic velocity lens model already used to demonstrate the traveltime interpolation.

Our first example is a homogeneous model with elliptical anisotropy. We considered P-waves with the relevant density-normalised elastic coefficients $A_{11} = A_{22} = 15.96 \, \mathrm{km^2/s^2}$ and $A_{33} = 11.4 \, \mathrm{km^2/s^2}$. Coarsely-gridded traveltime tables were computed analytically on a 100 m coarse grid. The geometrical spreading was computed on the coarse grid using Equation (8) and the coefficients from Equation (1). Subsequent trilinear interpolation was then carried out to obtain the spreading on a 10 m fine grid. The results were compared to the analytical solution (e.g. after Pšenčík and Teles, 1996). Figure 3 shows both the spreading itself and its relative errors. The median of the relative errors is 0.23 % and its maximum is 9.2 %. Please note in Figure 3, that the main contributions to the errors come from the trilinear interpolation. This is especially true in the region near the source where the wavefront curvature is strongest. This region is, however, of minor interest for migration.

In the next example we show the geometrical spreading resulting from the coarsely-gridded traveltimes for the triclinic lens model already used for the traveltime interpolation in the previous section. Again, the spreading was computed from the traveltime coefficients and the elasticity tensor at the coarse grid points with the 100 m spacing and tri-linearly interpolated onto the 10 m fine grid. Since no analytical solution exists for this model, and a suitable tool for the computation of geometrical spreading on a densely sampled 3-D grid is not available to us, the errors can not be quantified. As for the traveltimes we expect errors near the triplications of the wavefront in the centre of the model. Figure 4 shows the geometrical spreading for the whole model as well as a section through the triplicated wavefront region. Again, to obtain the correct coefficients in these regions, later-arrival traveltimes are required.

Numerous examples of the determination of geometrical spreading from traveltimes in isotropic media ranging from simple constant velocity gradient media to the highly complex Marmousi model are shown in Vanelle (2002) and illustrate the high accuracy of our technique in isotropic media. Since the coefficients that enter the spreading computation are formally the same for isotropic media as for anisotropic media,
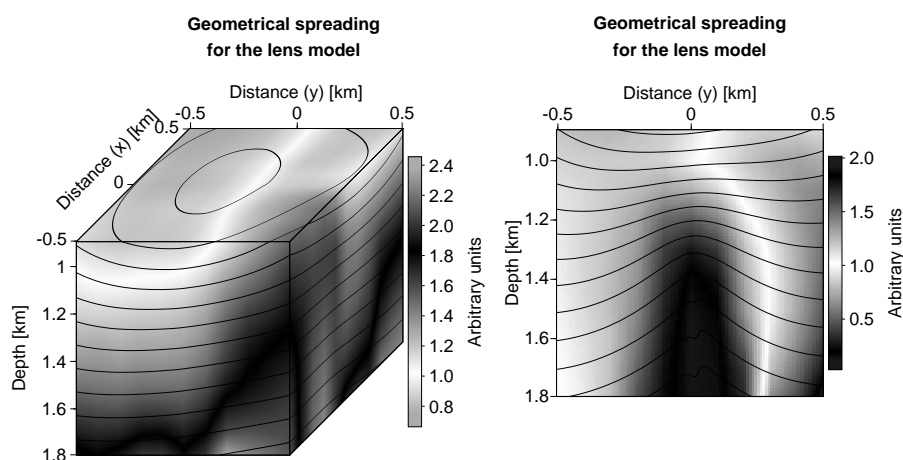
Figure 4: Geometrical spreading determined from traveltimes for a velocity lens model with a triclinic symmetry. The section on the right side cuts through a triplicated wavefront. In the blue centre region near the triplication the spreading values are wrong. To correctly determine the traveltime coefficients in these regions, later-arrivals are required. The shape of the isochrones in the centre of the model is caused by artifacts in the reference traveltimes.

the good performance of the method in isotropic models confirms its potential for anisotropic media.

CONCLUSIONS

We have presented a method for the determination of geometrical spreading for any wave type from coarsely-gridded traveltimes in 3D media with arbitrary anisotropy. The method is based on a second-order hyperbolic traveltime expression, the general NMO equation. The coefficients in this equation are directly linked to the geometrical spreading. The method is particularly suited for applications regarding amplitude preserving migration because the geometrical spreading is a key feature for this task. Since all required quantities can be computed on the fly from traveltime tables on coarse grids, the requirements in computer storage can be significantly reduced in comparison to amplitude preserving migration based on dynamic ray tracing. At the same time, the general NMO equation is a tool for the accurate and efficient interpolation of the stacking surface, including the interpolation between source positions.

A numerical example on the traveltime interpolation shows that the storage requirements can be reduced by a factor of 10^5 without significant loss in accuracy. Also, the interpolation is faster than traveltime generation using finite-difference eikonal solvers. The determination of geometrical spreading alone from coarsely-gridded traveltime tables was also demonstrated by examples. The reliability of the technique was proved with an example where an analytical solution exists. An additional example verifies the applicability of the method to more complex models.

PUBLICATIONS

Detailed results on the interpolation of traveltimes in isotropic media were published in Vanelle and Gajewski (2002a). The determination of geometrical spreading from traveltimes was introduced for isotropic media in Vanelle and Gajewski (1999). Gajewski et al. (2002) describe the traveltime-based strategy for amplitude preserving migration in isotropic media. More details are given in Vanelle and Gajewski (2001), Vanelle and Gajewski (2002b), and Vanelle (2002). Vanelle (2002) also discusses the extension of the method to anisotropy. Finally, Gajewski and Vanelle (2001) and Gajewski and Vanelle (2002) analyse the hyperbolic traveltime equation in terms of a generalised moveout formula.

ACKNOWLEDGEMENTS

REFERENCES

Buske, S. (2000). *Finite difference solution of the ray theoretical transport equation*. PhD thesis, Universität Frankfurt.

Červený, V. (2001). *Seismic Ray Theory*. Cambridge University Press.

Gajewski, D., Coman, R., and Vanelle, C. (2002). Amplitude preserving Kirchhoff migration: a traveltime based strategy. *Studia geophysica et geodaetica*, 46:193–211.

Gajewski, D. and Pšenčík, I. (1990). Vertical seismic profile synthetics by dynamic ray tracing in laterally varying layered anisotropic structures. *Journal of Geophysical Research*, 95:11,301–11,315.

Gajewski, D. and Vanelle, C. (2001). Extending the $T^2 - X^2$ method to 3-D heterogeneous media. In *Expanded Abstracts*, page AVO4.7. Soc. Expl. Geophys.

Gajewski, D. and Vanelle, C. (2002). Revisiting NMO again? In *Expanded Abstracts*, pages E–21. Eur. Assn. Expl. Geophys.

Geoltrain, S. and Brac, J. (1993). Can we image complex structures with first arrival traveltime? *Geophysics*, 58:564–575.

Hubral, P., Schleicher, J., and Tygel, M. (1992). Three-dimensional paraxial ray properties, Part 1: Basic relations. *Journal of Seismic Exploration*, 1:265–279.

Mensch, T. and Rasolofosaon, P. (1997). Elastic wave velocities in anisotropic media of arbitrary anisotropy – generalization of Thomsen's parameters ϵ, δ, and γ. *Geophysical Journal International*, 128:43–63.

Pusey, L. C. and Vidale, J. E. (1991). Accurate finite-difference calculation of WKBJ traveltimes and amplitudes. In *Expanded Abstracts*, pages 1513–1516. Soc. Expl. Geophys.

Pšenčík, I. and Teles, T. N. (1996). Point source radiation in inhomogeneous anisotropic structures. *Pure and Applied Geophysics*, 148:591–623.

Schleicher, J., Tygel, M., Ursin, B., and Bleistein, N. (2001). The Kirchhoff-Helmholtz integral for anisotropic elastic media. *Wave Motion*, pages 353–364.

Soukina, S. M., Gajewski, D., and Kashtan, B. M. (2001). Finite-difference perturbation method for 3-D anisotropic media. In *Expanded Abstracts*. Eur. Assn. Expl. Geophys.

Vanelle, C. (2002). *Traveltime-based True-amplitude Migration*. PhD thesis, University of Hamburg.

Vanelle, C. and Gajewski, D. (1999). Determining geometrical spreading from traveltimes. In *Expanded Abstracts*, page 1.56. Eur. Assn. Expl. Geophys.

Vanelle, C. and Gajewski, D. (2001). Determining the optimum migration aperture from traveltimes. *Journal of Seismic Exploration*, 10:205–224.

Vanelle, C. and Gajewski, D. (2002a). Second-order interpolation of traveltimes. *Geophysical Prospecting*, 50:73–83.

Vanelle, C. and Gajewski, D. (2002b). True amplitude migration weights from traveltimes. *Pure and Applied Geophysics*, 159:1583–1599.

Vidale, J. (1990). Finite-difference calculation of traveltimes in three dimensions. *Geophysics*, 55:521–526.

Vidale, J. and Houston, H. (1990). Rapid calculation of seismic amplitudes. *Geophysics*, 55:1504–1507.

Vinje, V., Iversen, E., and Gjøystdal, H. (1993). Traveltime and amplitude estimation using wavefront construction. *Geophysics*, 58:1157–1166.